HHS Public Access

Author manuscript

Neuroimage. Author manuscript; available in PMC 2019 February 15.

Published in final edited form as:

Neuroimage. 2018 February 15; 167: 342–353. doi:10.1016/j.neuroimage.2017.11.053.

Diffusion MRI and MR spectroscopy reveal microstructural and metabolic brain alterations in chronic mild stress exposed rats: A CMS recovery study

Ahmad Raza Khan[1], **Brian Hansen**[1], **Ove Wiborg**[1], **Christopher D. Kroenke**[2], and **Sune Nørhøj Jespersen**[1,3]

[1]Center of Functionally Integrative Neuroscience, Aarhus University Hospital, Aarhus, Denmark

[2]Advanced Imaging Research Center, Oregon Health & Science University, Portland, Oregon, United States

[3]Department of Physics and Astronomy, Aarhus University, Aarhus, Denmark

Abstract

Chronic mild stress (CMS) induced depression elicits several debilitating symptoms and causes a significant economic burden on society. High variability in the symptomatology of depression poses substantial impediment to accurate diagnosis and therapy outcome. CMS exposure induces significant metabolic and microstructural alterations in the hippocampus (HP), prefrontal cortex (PFC), caudate-putamen (CP) and amygdala (AM), however, recovery from these maladaptive changes are limited and this may provide negative effects on the therapeutic treatment and management of depression. The present study utilized anhedonic rats from the unpredictable CMS model of depression to study metabolic recovery in the ventral hippocampus (vHP) and microstructural recovery in the HP, AM, CP, and PFC. The study employed ^{1}H MR spectroscopy (^{1}H MRS) and in-vivo diffusion MRI (d-MRI) at the age of week 18 (week 1 post CMS exposure) week 20 (week 3 post CMS) and week 25 (week 8 post CMS exposure) in the anhedonic group, and at the age of week 18 and week 22 in the control group. The d-MRI data have provided an array of diffusion tensor metrics (FA, MD, AD, and RD), and fast kurtosis metrics (MKT, W_{L} and W_{T}). CMS exposure induced a significant metabolic alteration in vHP, and significant microstructural alterations were observed in the HP, AM, and PFC in comparison to the age match control and within the anhedonic group. A significantly high level of N-acetylaspartate (NAA) was observed in vHP at the age of week 18 in comparison to age match control and week 20 and week 25 of the anhedonic group. HP and AM showed significant microstructural alterations up to the age of week 22 in the anhedonic group. PFC showed significant microstructural alterations only at the age of week 18, however, most of the metrics showed significantly higher value at the age of week 20 in the anhedonic group. The significantly increased NAA concentration may indicate impaired catabolism due to astrogliosis or oxidative stress. The significantly increased W_{L} in the

*Corresponding Author: Sune Jespersen, CFIN/Dept. of Physics and Astronomy, Aarhus University, Building 10G, 5th Floor, Nørrebrogade 44, DK-8000 Århus C, Denmark, Phone +4578463334 / sune@cfin.au.dk.

AM and HP may indicate hypertrophy of AM and reduced volume of HP. Such metabolic and microstructural alterations could be useful in disease diagnosis and follow-up treatment intervention in depression and similar disorders.

Keywords

Chronic mild stress; diffusion MRI; Kurtosis; ^{1}H MRS; Amygdala; Hippocampus

Introduction

Chronic stress exposure contributes to illness in several debilitating diseases, such as cardiovascular disease, atherosclerosis (Steptoe and Kivimäki, 2012), diabetes (Grigsby et al., 2002), neurodegenerative diseases (Czéh et al., 2015; Janakiraman et al., 2016), and other mental disorders (McEwen and Gianaros, 2011; Wiborg, 2013). In addition to being detrimental to health, chronic stress causes poor quality of life and a general loss of productivity. Through these effects, chronic stress poses a significant economic burden on society (Ferrari et al., 2013). The absence of detectable pathological hallmarks and the variability in symptoms of depression represent a substantial impediment to accurate diagnosis and therapy outcome. Diagnosis of depression is based solely on duration and severity of symptoms as described in the Diagnosis and Statistical Manual V (DSM V) (American Psychiatric Association, 2013). Although the vast heterogeneity of symptoms also poses challenges in accurate modeling of depression in animal models, the unpredictable chronic mild stress (CMS) animal model is considered a realistic model of depression and demonstrates pertinent face validity (similar behavioral phenotypes as in the clinical symptom profile), predictive validity (similar response to clinically effective/ineffective treatment), etiological validity (triggering by similar events, which elicit human disorder) and construct validity (a loss of responsiveness to pleasant events, which is a core symptom of depression) (Wiborg, 2013; Willner, 1997). Chronic stress exposure induces significant microstructural and functional alterations in subcortical and cortical regions, especially in hippocampus (HP) (Henckens et al., 2015; Kalisch et al., 2006; Vestergaard-Poulsen et al., 2011), amygdala (AM) (Bourgin et al., 2015; Khan et al., 2016a; Roozendaal et al., 2009; Vyas et al., 2004), caudate-putamen (CP) (Dias-Ferreira et al., 2009; y Palacios et al., 2014) and prefrontal cortex (PFC) (McEwen and Gianaros, 2011; Radley et al., 2004).

Hippocampal atrophy reliably associates with depression and indicates cognitive aspects of behavioral impairments in animals (Anacker et al., 2015; Kalisch et al., 2006; Tse et al., 2014; Vyas et al., 2004) and humans (Kempton et al., 2011; Videbech and Ravnkilde, 2004). In contrast to HP, hypertrophy of AM is reliably detected after chronic stress exposure and may account for co-morbid anxiety symptoms (Khan et al., 2016a; Vyas et al., 2002), while reduced volume of CP after stress exposure is regarded as an indication of abnormal reward processing (Kumar et al., 2014; Sacchet et al., 2016; y Palacios et al., 2014). Similar to HP, CMS exposure also causes PFC atrophy, which is believed to affect higher cognitive processes, and the regulation of stress-induced hypothalamic-pituitary-adrenal (HPA) activity (Radley et al., 2006; Wilson et al., 2015). Moreover, differential response of dorsal HP (dHP) and ventral HP (vHP) was also demonstrated recently in the preclinical chronic

stress studies (Ballesteros et al., 2014; Sousa et al., 2000) and in the review articles (Bannerman et al., 2014; Fanselow and Dong, 2010). More specifically, changes in dHP are associated with poor spatial learning memory and changes in vHP with anxiety-like behaviors after CMS exposure (Bannerman et al., 2004; Conrad et al., 2016). This might be due to the fact that dHP receives multimodal sensory information from cortical regions, while vHP is closely linked to the AM and the Hypothalamic pituitary axis (HPA) (Bannerman et al., 2004; Bannerman et al., 2014). More recently, optogenetic approaches reveal stress induced behavioural abnormalities dependent on impaired function of specific brain regions and projection-specific alterations of neural networks (Chaudhury et al., 2013; Golden et al., 2016).

In spite of all these findings, the understanding of maladaptive responses of sensitive brain regions to stress and its potential reversibility remains limited. Better understanding of microstructural and metabolic recovery after CMS exposure could have great scientific value and mediate positive effects on the treatment and management of depression. Until now, only a limited number of clinical (Gong et al., 2011; Zhao et al., 2014) and preclinical studies (Bian et al., 2012; Gong et al., 2011; Sousa et al., 2000) have demonstrated recovery after microstructural and metabolic alterations. However, preclinical studies were limited to a specific brain region and/or the timeline for recovery was relatively short, such as 3 weeks (Vyas et al., 2004) and 6 weeks (Bian et al., 2012). Nonetheless, these studies demonstrated reversibility of some maladaptive forms of stress-related brain plasticity and indicate post stress exposure regulation (McEwen and Gianaros, 2011). Therefore, in the present study, we set out to explore the recovery of CMS induced microstructural and metabolic alterations using a longitudinal experimental design covering a period of 8 weeks post CMS exposure.

The present study aims to explore microstructural and metabolic alterations using diffusion MRI (d-MRI) and ^{1}H magnetic resonance spectroscopy (^{1}H MRS) in a group of rats exposed to unpredictable CMS exposure for eight weeks (from week 9 to week 17). To examine metabolic alterations in left vHP using in-vivo^{1}H MRS, and microstructural alterations using d-MRI scans were carried out post-CMS paradigm when the rats were 18 weeks (week 1 post CMS exposure), 20 weeks (week 3 post CMS exposure) and 25 weeks of age (week 8 post CMS exposure). ^{1}H MRS revealed significant metabolic changes in CMS animals at the age of week 18 with gradual normalization up to the age of week 25 (last time point). The d-MRI revealed significant microstructural alterations at the age of week 18, week 20, and week 22 in comparison to the age match control and among the anhedonic group at three time points, but no apparent microstructural alteration was observed at the age of week 25 (week 8 post CMS exposure) in comparison to the week 22 control and mean of the week 20 and week 25 of the anhedonic group. Such multimodal MRI studies provide better understanding of metabolic and microstructural recovery of CMS-induced depression, and helps identify which MRI methods and parameters could be useful for diagnosis and evaluation of treatment outcome in depression and similar disorders.

Materials and Methods

Animals, stress paradigm, and Sucrose consumption test

Sixteen adult, male, Long Evans rats (Janvier Labs, Denmark) were utilized in this longitudinal study. An illustration of the experimental design of the present study is shown in (Fig. 1a). Animals were exposed to a set of unpredictable chronic mild stressors such as one period of stroboscopic light, intermittent illumination, grouping, food or water deprivation; two periods of soiled cage, and no stress; and three periods of 45° cage tilting. Each stressor lasted for 10–14 hours as described previously (Varga et al., 2017; Wiborg, 2013).. All the animals had free access to food and tap water, except under food and water deprivation fourteen hours before a weekly (week 18–week 25) sucrose consumption test (SCT). Based on the SCT, CMS exposed animals were further identified as anhedonic or resilient, more specifically, whose sucrose consumption was reduced by more than 30% are defined as anhedonic and a reduced consumption of less than 10% are defined as stress resilient during the stress paradigm (Wiborg, 2013) (Supplementary Fig. 1 and Fig. 1b). Only anhedonic animals were included in this study to examine the metabolic recovery of vHP and microstructural recovery of the brain in the targeted region of interest (ROIs) from the age of week 18 to week 25. A group of (N=8) animals were identified as anhedonic, and an unexposed age-match group was included as control (N=8). Anhedonic rats were scanned in a preclinical MRI system at the ages of week 18, week 20, and week 25, and the age-match control group underwent the same scanning protocols at the ages of week 18 and week 22. Animal handling and experimentation were conducted in accordance with the national guidelines for animal research with the permission from Animal Experiments Inspectorate of the Danish Ministry of Food, Agriculture, and Fisheries, Denmark (2013-15-2934-00814).

In-vivo MRI

All MRI experiments were performed on a 9.4 T Bruker Biospec preclinical MRI system equipped with a BGA-12HP gradient set and a cross-coil combination of radiofrequency coils, with a 76 mm quadrature coil for excitation and a four element rat brain cryosurface coil for signal reception (Bruker Biospin, Ettlingen, Germany) as described in (Hansen et al., 2017). Rats were initially anesthetized with 4–5% isoflurane (gas anesthesia) for ~5 minutes and then placed on the bed of an animal holding system in the prone position. Subsequently, anaesthesia was maintained with 1.5–2.5% isoflurane mixed with air and oxygen throughout the experiment. Animal body temperature was monitored with a rectal probe connected to a physiological monitoring system, and maintained by a circulating warm water blanket under the animal bed. Respiration rate was monitored throughout the MRI procedures using the physiological monitoring system.

Anatomical Scans

High-resolution T2 weighted anatomical images were acquired in the coronal plane with a RARE (Rapid acquisition relaxation enhancement) sequence with TR/TE= 2832/14.5 ms and matrix size 380×380 to get 75μm in-plane resolution with 300 μm slice thickness and 38 slices to cover the whole brain. Saturation slices were placed in all three orthogonal

directions to reduce motion artefacts and to suppress signal from outside the brain. The total time for the in-vivo anatomical scan was 17.5 minutes.

^{1}H MRS

In-vivo ^{1}H MRS data was collected from left vHP using PRESS (Point resolved spectroscopy sequence) with TR/TE 5000/16 ms and 512 averages spanning 42 min of scan time. Anatomical images were used as reference images to position the volume of interest. Prior to the spectral acquisition, first and second order shims were adjusted for the voxel using the fast automatic shimming technique by mapping along projection (FASTMAP) scheme for optimal magnetic field homogeneity in the voxel (Pfeuffer et al., 2000; Tkáč et al., 2004). Automatic shim adjustment using FASTMAP ensures high spectral resolution. The quality of shim was assessed from the water signal linewidth. Spectra were acquired only after achieving <20 Hz water signal linewidth (~0.05 ppm). The water signal was suppressed with the variable power RF pulses with optimized relaxation delays (VAPOR) scheme combined with outer volume saturation (OVS). Zero and first order phase corrections were applied to all in-vivo spectra using the program LC model (Provencher, 2001). Subsequently, spectra were used to estimate metabolite concentrations by referencing a “basis set” obtained from in-vitro spectra (Provencher, 2001). This basis set allows quantification of the concentration of each metabolite. The TE for the in-vitro spectral acquisition was identical to the TE used to acquire the in-vivo spectra. The LC model analysis also outputs uncertainties of the metabolite concentration as Cramer-Rao lower bounds (CRLB), which establishes the accuracy of the metabolite concentration. The lower the value of CRLB, the higher the accuracy of the estimated concentration of metabolites. The present study considered only those metabolites having CRLB < 20%, for further statistical analysis, as this threshold is widely used in clinical (Basharat et al., 2015; Järnum et al., 2011) and preclinical studies (Kumar et al., 2012; Mlynárik et al., 2008; Tkáč et al., 2004).

d-MRI

In-vivo d-MRI data were acquired with a diffusion protocol consisting of a fast kurtosis acquisition scheme described previously (Hansen et al., 2017; Hansen et al., 2013; Hansen et al., 2014a; Hansen et al., 2015). In brief, data were acquired using a segmented EPI sequence (four segments) with parameters: diffusion times (δ/Δ) of 6ms/14ms, b-values 1.0 ms/μm^2 and 2.5 ms/μm^2 with three b=0 images and nine directions (Hansen and Jespersen, 2017). Other scan parameters were TR/TE=2237/27 ms, number of slices = 38, isotropic resolution = 300 μm, matrix size = 128×64. Twenty averages were acquired, resulting in a total scan time of 1hr and 10 minutes. The brain slices have identical position to those of the anatomical scan. To reduce motion artefacts during the MRI experiments, saturation slices were placed in all the three orthogonal imaging planes.

Anatomical images from each brain were inspected visually for any gross changes in anatomy and diffusion weighted images were inspected for any abnormal signal behaviour or image artefacts prior to pre-processing of the d-MRI data. The d-MRI data of one animal from the anhedonic group at the age of week 18 and week 20 and one animal from the control group at the age of week 18 and week 22 were found to have motion artefacts and

were excluded from the study. A total of 35 brains (7 at each time point for anhedonic and control groups) were analysed for the present study.

Pre-processing of d-MRI data

All diffusion-weighted images were registered to the corresponding non-diffusion-weighted (b0) images using affine transformation in Matlab to correct any misalignment in the diffusion-weighted images. Diffusion data was further corrected for denoising in Matlab using Marchenko-Pasteur principal component analysis (Veraart et al., 2016). Following denoising correction, Gibbs ringing artefacts were corrected using an approach based on local, sub-voxel-shifts described recently (Kellner et al., 2015). Gibbs ringing correction was also implemented in Matlab (The Mathworks, Natick, MA). Prior to parameter estimation data was again inspected visually for any misalignment with b=0 images or any other artefacts.

Parameter estimation and ROI placement

Pre-processed d-MRI data was subjected to parameter estimation to compute an array of d-MRI based metrics. Traditional d-MRI metrics (FA, MD, AD, and RD (Basser, 1995, 1997), and kurtosis tensor metrics (MKT, W_L and W_T) of fast and axisymmetric diffusion kurtosis imaging (DKI) (Hansen et al., 2013; Hansen et al., 2014b; Hansen et al., 2015; Hansen et al., 2016) were considered. The axisymmetric DKI parameters reduces the number of parameters from 20 to 8 based on the assumption of axial symmetry described elsewhere (Hansen et al., 2016) and are clinically feasible (Næss-Schmidt et al., 2017). The study explored four different regions of interest (ROIs) of the brain, viz. AM, PFC, CP, and HP. Due to differential microstructural alterations observed in the dorsal and ventral HP in some studies, HP was further subdivided into dHP and vHP. All regions of interest (ROIs) considered in this study were delineated according to the coordinates specified in the rat brain atlas and in previous literature (Fig. 2) (Bannerman et al., 2003; Bourgin et al., 2015; Paxinos and Watson, 1998) on the b=0 images of the d-MRI data. For example, dHP was defined as −3.10 to −4.28 mm and vHP was −4.60 to −8.82 mm (Fig. 3) relative to bregma (Bannerman et al., 2004; Christensen et al., 2010).

Statistical analysis

All statistical test procedures applied in the present study are presented in Table 1. The presence of significant changes in the anhedonic group over different time points was assessed using a linear mixed effects model with animals as random effects (allowing for inter-subject variability) and group (each time points of control and anhedonic group) as a fixed effect. For SCT, weekly (week 18–week 25) sucrose consumption data and for MRI experiment each time point of the anhedonic (at week 18, week 20 and week 25) and control (at week 18, and week 22) considered as group. Confidence intervals (CI) (95%) were computed using the ‘coefCI’ function in Matlab, providing fixed effect size and variability. The level of significance was assessed using an F-test as described previously (Khan et al., 2016a) and post hoc tests were used to assess statistically significant differences between time point pairs (p^{12}, p^{13}, p^{23}) of the anhedonic group (Table 1).

Student's t-tests were applied to test the level of significance in between control and anhedonic groups at the age of week 18 (**#)**, and between anhedonic at week 20 and mean of the control at week 18 and week 22 (considered as control at week 20) (€). Likewise, mean of the anhedonic group at week 20 and 25 was considered as week 22 and compared with control at week 22 to test the level of significance (†). A paired t-test was applied to test the level of significance between control group at week 18 and week 22 ($). All the p-values were corrected for false discovery rate (FDR), of multiple testing across all measures (Benjamini and Hochberg, 1995; Noble, 2009) in Matlab (Natick, USA), and only p-values surviving the level of significant difference ($p<0.05$) after FDR correction are reported here.

Results

All anatomical images were visually inspected for any gross morphological changes, specifically in the target ROIs (Fig. 2). The SCT in the anhedonic group indicates a significant recovery of sucrose consumption from week 21 to week 25 in comparison to week 18 ($p<0.001$) (Fig 1b). Although MR parameters employed in the present study and SCT both indicate recovery, however, there were no strong correlation between SCT and any of the MR parameters.

^{1}H MRS

Quantification of metabolite ratios obtained from the processed spectra using LC model (Fig. 3) revealed significant increase in metabolite levels (normalized by total creatinine (tCr) concentration). N-acetylaspartate (NAA/tCr) was significantly higher at week 18 in comparison to the control (# $p<0.05$), and in comparison to the week 20 (*$p^{12}<0.05$) and week 25 (*$p^{13}< 0.05$) of the anhedonic group (Fig. 4, Table 2). The inositol concentration ratio (Ins/tCr) at week 20 in the anhedonic group was also significantly high in comparison to the mean of Ins at week 18 and week 22 of the control group (€ $p<0.05$). Likewise, the mean of inositol at week 20 and week 25 of the anhedonic group was significantly higher compared to the control at week 22 (†$p<0.05$). The ratio of glutamine and glutamate combined (Glu+Gln) was also altered in the anhedonic group, although it did not survive FDR correction. Similarly, NAA+ NAAG and glutathione (GSH/tCr) ratios were markedly higher at week 18 in the anhedonic group compared to age match controls, although this effect was not significant after FDR correction. At the age of week 25, most of the metabolites from the anhedonic group did not show any apparent differences in comparison to the control at the age of week 22.

d-MRI

There were no apparent artefacts or abnormalities in any of the parameter maps (Fig. 5) of d-MRI data and anatomical data of the brains from control and anhedonic groups.

Diffusion tensor metrics (MD, AD, RD, and FA)

Diffusion tensor metrics revealed significant microstructural alterations in HP and AM (Fig. 6(a)–(d)). The anhedonic group showed significantly higher FA (*$p^{23}<0.05$) at the age of week 20 in comparison to week 25. FA was also significantly high in AM at week 20 in comparison to the mean of control at week 18 and week 22 (€ $p<0.05$) (Fig. 6(d), Table 2).

The mean of AD at the age of week 20 and week 25 in the HP of the anhedonic group was significantly higher (†p<0.05) in comparison to the control at week 22. A common trend of higher values of diffusion tensor metrics at week 20 was observed in most of the ROIs. Wider CIs were observed in all diffusion tensor metrics of the anhedonic group in all the four ROIs, and PFC showed wider CI in comparison to other ROIs. A similar observation in the PFC was also noticed in a previous study on the CMS model of depression (Khan et al., 2016a; Khan et al., 2016b).

Kurtosis tensor metrics (MKT, W_L and W_T)

Tensor-based kurtosis metrics also showed significant alterations in all the ROIs except CP (Fig. 7(a)–(c)). A significantly higher W_L in the PFC and W_T in the HP was observed in the anhedonic group at week 18 in comparison to the age match control group (# p<0.05) (Fig. 7(b), 7(c)). Similar to the diffusion tensor metrics, AM and HP also showed significantly higher W_L in the anhedonic group at the age of week 20 in comparison to the mean of control at week 18 and week 22 (€ p<0.05) and also within the anhedonic group at week 18 (*p^{12}<0.05) and week 25 (*p^{23}<0.05) (Fig. 7(b), Table 2). MKT did not change significantly in the anhedonic group. Although, similar to other diffusion tensor metrics, higher value of kurtosis tensor metrics (MKT, W_L, and W_T) were also evident at the age of week 20 in the anhedonic group.

We did not find any significant variation in any of the diffusion tensor and kurtosis tensor metrics in the control group in any of the four ROIs at the age of week 18 and week 22.

Diffusion tensor and kurtosis tensor metrics in dHP and vHP

Next, we examined the microstructural alterations in dHP and vHP in order to explore local effects within the HP. Differential microstructural alterations were observed in dHP and vHP region (Fig. 8(a)) after CMS exposure (Fig. 8(b–h)). A significantly higher W_L in the vHP was observed in comparison to the mean of control at week 18 and week 22 (€ p<0.05) and also in comparison to the week 18 and week 25 of the anhedonic group (**p<0.05) (Fig. 8(g)). The mean of AD over the ages of week 20 and week 25 was significantly higher in both dHP and vHP of the anhedonic group in comparison to the control at the age of week 22 (†p<0.05) (Fig. 8(d)). The only significant difference within the control group (over the ages of week 18 and week 22) was observed in FA of dHP ($p<0.05) (Fig. 8(b)). Similar to the higher values of diffusion tensor and kurtosis parameters at the age of week 20 in the anhedonic group in almost all the ROIs, vHP showed higher FA, AD, and W_L, while dHP showed higher RD, W_T, and W_L at week 20 in the anhedonic group, however, these differences were not statistically significant.

Discussion

Altered levels of cerebral metabolites are characteristic for depression and may be associated with microstructural alterations (Hasler and Northoff, 2011; Varga et al., 2017); however, to date, no objective biomarker has yet qualified as a pathological hallmark of depression. A multimodal in-vivo approach is advantageous to study disease progression/regression to reveal metabolic and microstructural alterations, in particular in depression due to its varying

symptoms. ^{1}H MRS is widely accepted as a clinical tool and can substantiate specific information about neurometabolites, which could help in diagnosis and therapy outcome (Hasler and Northoff, 2011). In the present study ^{1}H MRS data revealed significantly higher NAA after CMS exposure. In contrast to this observation, previous studies have reported reduced NAA levels in psychiatric disorders (Järnum et al., 2011; Kumar et al., 2014; Sapolsky, 2000; Xi et al., 2011). Such findings were tentatively interpreted to be associate with a reduction in neuronal cell number, although reduced number of adult-born neurons were reported in depressed patient only in dentate gyrus recently (Boldrini et al., 2013), however, post-mortem studies have shown no significant reduction in total neuronal cell numbers in these disorders (Manji et al., 2000; Rajkowska, 2000). In agreement with the present findings, a markedly higher NAAG/tCr level was observed in a study employing a similar CMS paradigm (y Palacios et al., 2011); however, no other significant alterations in metabolite levels were observed in the anhedonic group in comparison to control. A significantly higher NAA/tCr in the anhedonic group at the age of week 18 may suggest impaired catabolism of NAA, as NAA is catabolized in astrocytes and oligodendrocytes, and may be affected by astrogliosis (Aston et al., 2005; Baslow, 2003; Stockmeier et al., 2004). Besides cellular alterations, other studies also reported higher NAA indicating oxidative stress (Surendran and Bhatnagar, 2011). A markedly higher level of glutathione (GSH/tCr) an important antioxidant of the cells, at the age of week 18 although not significant (n.s), in the anhedonic group also indicates oxidative stress post-CMS exposure (Arnsten, 2009; McEwen and Stellar, 1993). A marked reduction in (Gln + Glu)/tCr observed in the present study (n.s) is also supported by previous studies on humans (Järnum et al., 2011) and animal models (Kumar et al., 2012) and suggests impaired neurotransmission in CMS induced depression. The present study also showed significantly higher inositol level at 20 weeks of age in comparison to the age match controls, which might indicate abnormal osmoregulation in vHP. In support of this finding, Kumar et al. (2012) also reported higher inositol after CMS exposure in the HP (Kumar et al., 2012). However, most of the metabolic alterations in the anhedonic group were normalized at the age of week 25 in the present study.

In addition to the metabolic alterations, d-MRI based diffusion tensor and kurtosis metrics revealed significant microstructural alterations in most of the ROIs investigated. One of the main findings of the present study is significantly higher W_{L} in the AM and HP at the age of week 20 of the anhedonic group. This might relate to CMS induced hypertrophy in the AM, which is reported in studies based on humans (Drevets et al., 2008; Stockmeier et al., 2004) and animals (Khan et al., 2016a; Mitra et al., 2005; Vyas et al., 2006). In addition to hypertrophy in the AM, demyelination and astrogliosis have also been reported in post-mortem brain tissue (Rajkowska, 2000; Stockmeier et al., 2004) as well as in preclinical depression models (Khan et al., 2016a; McHugh et al., 2004; Mitra et al., 2005; Roozendaal et al., 2009). Although it is challenging to interpret DKI metrics in terms of tissue microstructure, a significantly higher W_{L} and markedly enhanced MD could be considered consistent with a higher neurite density in the AM, which matches our previous findings (Khan et al., 2016a). Similar findings were reported by y Palacios et al., (2014), in which significantly higher RD and moderately higher AD in the amygdala of the unpredictable CMS model of depression was observed, but no significant alterations in any kurtosis measure were observed in comparison to the controls (y Palacios et al., 2014). We did not

observe any significant changes of RD, MD, and MKT measures in the AM at the age of week 18 in the anhedonic group. This observation is in contrast to our previous finding of significantly lower MD and higher MKT in the AM of unpredictable CMS rat brain (Khan et al., 2016a). This significant alteration in AM of the previous study was associated with a significantly higher neurite density in the AM of stressed rats in comparison to controls. This differential effect in AM may be due to the different strain of rats employed in the two studies (Wistar in the previous and Long Evans in the present study). Such differential effects have previously been observed in studies employing a similar stress paradigm on different rat strains. For example, one study observed significantly higher FA and lower MD in Sprague Dawley (SD) rats, while a F344 rat strain did not exhibit such microstructural alterations (Magalhães et al., 2017). In another study, a significantly higher volume of AM was reported in F344 rats but not in SD rats after CMS exposure (Bourgin et al., 2015). A similar CMS model of depression has demonstrated high variation and higher faecal corticosterone level in the anhedonic rats (Christiansen et al., 2012). Such differential metabolite, microstructural and volume alterations parallel the immense heterogeneity of symptoms of depression. We also observed higher CI in most of the diffusion parameters analysed from the anhedonic group in both the present and the previous studies (Khan et al., 2016a; Khan et al., 2017). The higher CI also indicates a differential recovery rate after CMS exposure in the anhedonic group and may reflect the heterogeneity of symptoms of depression widely reported in animals (Khan et al., 2016a; Khan et al., 2017; Wiborg, 2013; Wilson et al., 2015) and humans (Zhao et al., 2016; Zhao et al., 2014)

Another significant finding of the present study is high W_T in HP at the age of week 18 in the anhedonic group. y Palacios et al. (2011) reported significantly lower radial kurtosis and mean kurtosis in HP of the unpredictable CMS model (y Palacios et al., 2011). However, as discussed previously, these contrasting alterations might be due to the different scan time or rat strains employed, indicative of differential but significant vulnerability of the HP to stress. A significant alteration of W_L in PFC at the age of week 18 was also observed in the anhedonic group. HP and PFC are considered to be among the most sensitive regions of the brain to CMS exposure and a differential effect in the dendritic architecture in sub-regions of HP and PFC have also been reported widely in different stress paradigms (Bannerman et al., 2004; Czéh et al., 2015; McEwen et al., 2015; Radley et al., 2004; Radley et al., 2005; Vestergaard-Poulsen et al., 2011). The present study also examined HP sub-regions dHP and vHP, which demonstrated higher FA and significantly higher W_L only in vHP at the age of week 20 may be possibly related to the CMS induced anxiety (Willner, 2016). This also suggests that the HP shows differential microstructural alterations in ventral and dorsal regions. A marked dendritic atrophy in cornu ammonis 3 (CA3) and dentate gyrus has been widely reported in studies employing stress paradigms (Cohen et al., 2014; Conrad et al., 2016; Henckens et al., 2015). However, we have not examined these hippocampal sub-regions, as they cannot be reliably delineated in our d-MRI data.

We also compared the mean values of the parameters at week 18 and week 22 of the control group to compare with anhedonic at week 20 and week 20 and week 25 from the anhedonic group with a control group at the age of week 22, assuming that microstructural changes were approximately linear between two time points of the control and anhedonic group. FA was significantly higher in the AM at week 20 in comparison to the mean of control at week

18 and week 22 and AD was significantly higher in the HP in comparison to control at the age of week 22. Anacker et al. 2017 reported positive correlation of FA in the AM with social avoidance score in the anhedonic group (Anacker et al., 2015), and Kumar et al. (2014) reported higher AD in left HP in comparison to controls after CMS exposure, while we observed higher AD in HP at the age of week 20 and week 25 in the anhedonic group. However, we have not examined lateral effects of CMS exposure on the brain. Furthermore, our analysis in HP reveal a significant alteration of AD in dHP and vHP. These alterations signify that only HP show persistent microstructural alterations lasting until week 22 in comparison to the age-match control. This is in contrast to Vyas et al. (2004), where it was shown that hypertrophy in the AM lasts longer than HP (Vyas et al., 2004). This might be due to the differential effect and rate of CMS recovery in different strains of animals or even differences in the experimental protocol or severity of stress. Additionally, higher AD in the HP at the age of week 20 could be associated with reduced volume of HP which is also considered as a hallmark of depression (Kempton et al., 2011). Nonetheless, a visual comparison with control at the age of week 22 with anhedonic at the age of week 25 reveals no marked variation in most of the diffusion parameters. These observations suggest that in the anhedonic group, by the age of week 25, most of the microstructural alterations have normalized to the control level. Our multimodal approach provides a better understanding of the dynamics of CMS based metabolic and microstructural alterations and indicates that clinically feasible spectroscopy and d-MRI methods produce markers of metabolic and microstructural alterations in the, stress sensitive regions of the brain. Our findings therefore suggest that spectroscopy and diffusion kurtosis methods may have clinical applications in the study/diagnosis of depression.

Limitations

The foremost limitation of the present study is the absence of control group MRI experiments at the same time points as the anhedonic groups, however, an assumption of linear metabolic and microstructural alterations between two time points allow us to compare the control and anhedonic group at week 20 and week 22. Another limitation of the present study is the absence of immunohistological tests at each time point of the CMS recovery is lacking and that could provide a great deal of information regarding specific microstructural alterations of the brain tissue to support the d-MRI based microstructural alterations. Although immunohistological test considered as gold standard for specific microstructure, however, needs extensive labour and above all invasive in nature. Nonetheless, preclinical studies have the advantage to use ex-vivo MRI along with immunohistological tests to support MRI based findings and may employed in the future studies.

Conclusion

We found significant microstructural and metabolic alterations in vHP using d-MRI and ^{1}H MRS, indicating abnormal NAA metabolism and impaired neurotransmission of stressed rats, possibly related to the CMS induced anxiety. Diffusion MRI based microstructural alterations in AM, HP, and PFC in CMS induced depression model of rats underscore the vital role of these brain regions in depression. ^{1}H MRS based metabolic alterations and d-

MRI based significant microstructural alterations interrogated with kurtosis tensor metrics and DTI parameters could be useful in disease diagnosis and follow-up treatment intervention.

Supplementary Material

Refer to Web version on PubMed Central for supplementary material.

Acknowledgments

Lundbeck Foundation R83-A7548 and R253-2017-215. Danish Ministry of Science, Technology and Innovation's University Investment Grant (MIND Lab, Grant no. 0601-01354B), and NIH 1R01EB012874-01. Danish Research Council's Infrastructure program, the Velux Foundations, and the Department of Clinical Medicine, AU.

Abbreviations

^{1}H MRS	^{1}H Magnetic resonance spectroscopy
AD	Axial diffusivity
AM	Amygdala
CA3	Cornu ammonis 3
CI	Confidence intervals
CMS	Chronic mild stress
CP	Caudate putamen
CRLB	Cramer-Rao lower bounds
dHP	dorsal hippocampus
d-MRI	diffusion MRI
DSM V	Diagnosis and Statistical Manual V
FA	Fractional anisotropy
FASTMAP	Fast automatic shimming technique by mapping along projection
FDR	false discovery rate
Glu	Glutamate
Gln	Glutamine
GSH	Glutathione
HP	Hippocampus
HPA	Hypothalamic pituitary axis
Ins	Inositol

MD	Mean Diffusivity
MKT	Mean kurtosis tensor
NAA	N-acetyl aspartate
NAAG	N-acetyl aspartyl glutamate
OVS	Outer volume saturation
PFC	Prefrontal cortex
PRESS	Point resolved spectroscopy sequence
RARE	Rapid acquisition relaxation enhancement
RD	Radial diffusivity
ROIs	Region of interest
SCT	Sucrose consumption test
SD	Sprague Dawley
VAPOR	variable power RF pulses with optimized relaxation delays
vHP	ventral hippocampus
W_L	Axial kurtosis tensor
W_T	Radial kurtosis tensor

References

American Psychiatric Association. Diagnostic and statistical manual of mental disorders. 5. Washington, DC: 2013.

Anacker C, Scholz J, O'Donnell KJ, Allemang-Grand R, Diorio J, Bagot RC, Nestler E, Hen R, Lerch JP, Meaney MJ. Neuroanatomical differences associated with stress susceptibility and resilience. Biological psychiatry. 2015

Arnsten AF. Stress signalling pathways that impair prefrontal cortex structure and function. Nature Reviews Neuroscience. 2009; 10:410–422. [PubMed: 19455173]

Aston C, Jiang L, Sokolov B. Transcriptional profiling reveals evidence for signaling and oligodendroglial abnormalities in the temporal cortex from patients with major depressive disorder. Molecular psychiatry. 2005; 10:309–322. [PubMed: 15303102]

Ballesteros CI, de Oliveira Galvão B, Maisonette S, Landeira-Fernandez J. Effect of dorsal and ventral hippocampal lesions on contextual fear conditioning and unconditioned defensive behavior induced by electrical stimulation of the dorsal periaqueductal gray. PloS one. 2014; 9:e83342. [PubMed: 24404134]

Bannerman D, Grubb M, Deacon R, Yee B, Feldon J, Rawlins J. Ventral hippocampal lesions affect anxiety but not spatial learning. Behavioural brain research. 2003; 139:197–213. [PubMed: 12642189]

Bannerman D, Rawlins J, McHugh S, Deacon R, Yee B, Bast T, Zhang WN, Pothuizen H, Feldon J. Regional dissociations within the hippocampus—memory and anxiety. Neuroscience & Biobehavioral Reviews. 2004; 28:273–283. [PubMed: 15225971]

Bannerman DM, Sprengel R, Sanderson DJ, McHugh SB, Rawlins JNP, Monyer H, Seeburg PH. Hippocampal synaptic plasticity, spatial memory and anxiety. Nature Reviews Neuroscience. 2014; 15:181–192. [PubMed: 24552786]

Basharat M, Payne GS, Morgan VA, Parker C, Dearnaley D, deSouza NM. TE= 32 ms vs TE= 100 ms echo-time 1H-magnetic resonance spectroscopy in prostate cancer: Tumor metabolite depiction and absolute concentrations in tumors and adjacent tissues. Journal of Magnetic Resonance Imaging. 2015; 42:1086–1093. [PubMed: 26258905]

Baslow MH. N-acetylaspartate in the vertebrate brain: metabolism and function. Neurochemical research. 2003; 28:941–953. [PubMed: 12718449]

Basser PJ. Inferring microstructural features and the physiological state of tissues from diffusion-weighted images. NMR in Biomedicine. 1995; 8:333–344. [PubMed: 8739270]

Basser PJ. New Histological and Physiological Stains Derived from Diffusion-Tensor MR Images. Annals of the New York Academy of Sciences. 1997; 820:123–138. [PubMed: 9237452]

Benjamini Y, Hochberg Y. Controlling the false discovery rate: a practical and powerful approach to multiple testing. Journal of the royal statistical society. Series B (Methodological). 1995:289–300.

Bian Y, Pan Z, Hou Z, Huang C, Li W, Zhao B. Learning, memory, and glial cell changes following recovery from chronic unpredictable stress. Brain research bulletin. 2012; 88:471–476. [PubMed: 22537595]

Boldrini M, Santiago AN, Hen R, Dwork AJ, Rosoklija GB, Tamir H, Arango V, Mann JJ. Hippocampal granule neuron number and dentate gyrus volume in antidepressant-treated and untreated major depression. Neuropsychopharmacology. 2013; 38:1068. [PubMed: 23303074]

Bourgin J, Cachia A, Boumezbeur F, Djemaï B, Bottlaender M, Duchesnay E, Mériaux S, Jay T. Hyper-responsivity to stress in rats is associated with a large increase in amygdala volume. A 7T MRI study. European Neuropsychopharmacology. 2015; 25:828–835. [PubMed: 25823695]

Chaudhury D, Walsh JJ, Friedman AK, Juarez B, Ku SM, Koo JW, Ferguson D, Tsai HC, Pomeranz L, Christoffel DJ. Rapid regulation of depression-related behaviors by control of midbrain dopamine neurons. Nature. 2013; 493:532. [PubMed: 23235832]

Christensen T, Bisgaard C, Nielsen HB, Wiborg O. Transcriptome differentiation along the dorso–ventral axis in laser-captured microdissected rat hippocampal granular cell layer. Neuroscience. 2010; 170:731–741. [PubMed: 20667465]

Christiansen S, Bouzinova E, Palme R, Wiborg O. Circadian activity of the hypothalamic–pituitary–adrenal axis is differentially affected in the rat chronic mild stress model of depression. Stress. 2012; 15:647–657. [PubMed: 22217141]

Cohen H, Kozlovsky N, Matar MA, Zohar J, Kaplan Z. Distinctive hippocampal and amygdalar cytoarchitectural changes underlie specific patterns of behavioral disruption following stress exposure in an animal model of PTSD. European Neuropsychopharmacology. 2014; 24:1925–1944. [PubMed: 25451698]

Conrad CD, Ortiz JB, Judd JM. Chronic Stress and Hippocampal Dendritic Complexity: Methodological and Functional Considerations. Physiology & Behavior. 2016

Czéh B, Varga ZKK, Henningsen K, Kovács GL, Miseta A, Wiborg O. Chronic stress reduces the number of GABAergic interneurons in the adult rat hippocampus, dorsal-ventral and region-specific differences. Hippocampus. 2015; 25:393–405. [PubMed: 25331166]

Dias-Ferreira E, Sousa JC, Melo I, Morgado P, Mesquita AR, Cerqueira JJ, Costa RM, Sousa N. Chronic stress causes frontostriatal reorganization and affects decision-making. Science. 2009; 325:621–625. [PubMed: 19644122]

Drevets WC, Price JL, Furey ML. Brain structural and functional abnormalities in mood disorders: implications for neurocircuitry models of depression. Brain structure and function. 2008; 213:93–118. [PubMed: 18704495]

Fanselow MS, Dong HW. Are the dorsal and ventral hippocampus functionally distinct structures? Neuron. 2010; 65:7–19. [PubMed: 20152109]

Ferrari AJ, Charlson FJ, Norman RE, Patten SB, Freedman G, Murray CJ, Vos T, Whiteford HA. Burden of depressive disorders by country, sex, age, and year: findings from the global burden of disease study 2010. PloS one. 2013:e1001547.

Golden SA, Heshmati M, Flanigan M, Christoffel DJ, Guise K, Pfau ML, Aleyasin H, Menard C, Zhang H, Hodes GE. Basal forebrain projections to the lateral habenula modulate aggression reward. Nature. 2016; 534:688–692. [PubMed: 27357796]

Gong Q, Wu Q, Scarpazza C, Lui S, Jia Z, Marquand A, Huang X, McGuire P, Mechelli A. Prognostic prediction of therapeutic response in depression using high-field MR imaging. NeuroImage. 2011; 55:1497–1503. [PubMed: 21134472]

Grigsby AB, Anderson RJ, Freedland KE, Clouse RE, Lustman PJ. Prevalence of anxiety in adults with diabetes: a systematic review. Journal of psychosomatic research. 2002; 53:1053–1060. [PubMed: 12479986]

Hansen B, Jespersen SN. Recent developments in fast kurtosis imaging. Frontiers in Physics. 2017; 5:40.

Hansen B, Khan AR, Shemesh N, Lund TE, Sangill R, Eskildsen SF, Ostergaard L, Jespersen SN. White matter biomarkers from fast protocols using axially symmetric diffusion kurtosis imaging. NMR Biomed. 2017:e3741. n/a.

Hansen B, Lund TE, Sangill R, Jespersen SN. Experimentally and computationally fast method for estimation of a mean kurtosis. Magn Reson Med. 2013; 69:1754–1760. [PubMed: 23589312]

Hansen B, Lund TE, Sangill R, Jespersen SN. Erratum: Hansen, Lund, Sangill, and Jespersen. Experimentally and Computationally Fast Method for Estimation of a Mean Kurtosis. Magnetic Resonance in Medicine, 69: 1754–1760, (2013). Magnetic Resonance in Medicine. 2014a; 71:2250–2250.

Hansen B, Lund TE, Sangill R, Jespersen SN. Erratum: Hansen, Lund, Sangill, and Jespersen. Experimentally and Computationally Fast Method for Estimation of a Mean Kurtosis, Magnetic Resonance in Medicine 69: 1754–1760 (2013). Magnetic Resonance in Medicine. 2014b; 71:2250–2250.

Hansen B, Lund TE, Sangill R, Stubbe E, Finsterbusch J, Jespersen SN. Experimental considerations for fast kurtosis imaging. Magn Reson Med. 2015; doi: 10.1002/mrm.26055

Hansen B, Shemesh N, Jespersen SN. Fast imaging of mean, axial and radial diffusion kurtosis. NeuroImage. 2016; 142:381–393. [PubMed: 27539807]

Hasler G, Northoff G. Discovering imaging endophenotypes for major depression. Molecular psychiatry. 2011; 16:604–619. [PubMed: 21602829]

Henckens MJ, van der Marel K, van der Toorn A, Pillai AG, Fernández G, Dijkhuizen RM, Joëls M. Stress-induced alterations in large-scale functional networks of the rodent brain. NeuroImage. 2015; 105:312–322. [PubMed: 25462693]

Janakiraman U, Manivasagam T, Thenmozhi AJ, Essa MM, Barathidasan R, SaravanaBabu C, Guillemin GJ, Khan MA. Influences of chronic mild stress exposure on motor, non-motor impairments and neurochemical variables in specific brain areas of MPTP/probenecid induced neurotoxicity in mice. PloS one. 2016; 11:e0146671. [PubMed: 26765842]

Järnum H, Eskildsen SF, Steffensen EG, Lundbye-Christensen S, Simonsen CW, Thomsen IS, Fründ ET, Théberge J, Larsson EM. Longitudinal MRI study of cortical thickness, perfusion, and metabolite levels in major depressive disorder. Acta Psychiatrica Scandinavica. 2011; 124:435–446. [PubMed: 21923809]

Kalisch R, Schubert M, Jacob W, Keßler MS, Hemauer R, Wigger A, Landgraf R, Auer DP. Anxiety and hippocampus volume in the rat. Neuropsychopharmacology. 2006; 31:925–932. [PubMed: 16192979]

Kellner E, Dhital B, Kiselev VG, Reisert M. Gibbs-ringing artifact removal based on local subvoxel-shifts. Magnetic Resonance in Medicine. 2015

Kempton MJ, Salvador Z, Munafò MR, Geddes JR, Simmons A, Frangou S, Williams SC. Structural neuroimaging studies in major depressive disorder: meta-analysis and comparison with bipolar disorder. Archives of general psychiatry. 2011; 68:675–690. [PubMed: 21727252]

Khan AR, Chuhutin A, Wiborg O, Kroenke CD, Nyengaard JR, Hansen B, Jespersen SN. Biophysical modeling of high field diffusion MRI demonstrates micro-structural aberration in chronic mild stress rat brain. NeuroImage. 2016a; 142:421–430. [PubMed: 27389790]

Khan AR, Chuhutin A, Wiborg O, Kroenke CD, Nyengaard JR, Hansen B, Jespersen SN. Summary of high field diffusion MRI and microscopy data demonstrate microstructural aberration in chronic mild stress rat brain. Data in Brief. 2016b; 8:934–937. [PubMed: 27508246]

Khan AR, Kroenke CD, Wiborg O, Chuhutin A, Nyengaard JR, Hansen B, Jespersen SN. Differential microstructural alterations in rat cerebral cortex in a model of chronic mild stress depression. 2017 Submitted.

Kumar A, Yang S, Ajilore O, Wu M, Charlton R, Lamar M. Subcortical biophysical abnormalities in patients with mood disorders. Molecular psychiatry. 2014; 19:710–716. [PubMed: 23877833]

Kumar BH, Mishra SK, Rana P, Singh S, Khushu S. Neurodegenerative evidences during early onset of depression in CMS rats as detected by proton magnetic resonance spectroscopy at 7T. Behavioural brain research. 2012; 232:53–59. [PubMed: 22449862]

Magalhães R, Bourgin J, Boumezbeur F, Marques P, Bottlaender M, Poupon C, Djemaï B, Duchesnay E, Mériaux S, Sousa N. White matter changes in microstructure associated with a maladaptive response to stress in rats. Translational Psychiatry. 2017; 7:e1009. [PubMed: 28117841]

Manji HK, Moore GJ, Rajkowska G, Chen G. Neuroplasticity and cellular resilience in mood disorders. Molecular psychiatry. 2000; 5:578–593. [PubMed: 11126389]

McEwen BS, Gianaros PJ. Stress-and allostasis-induced brain plasticity. Annual review of medicine. 2011; 62:431.

McEwen BS, Gray JD, Nasca C. Recognizing resilience: Learning from the effects of stress on the brain. Neurobiology of stress. 2015; 1:1–11. [PubMed: 25506601]

McEwen BS, Stellar E. Stress and the individual: mechanisms leading to disease. Archives of internal medicine. 1993; 153:2093–2101. [PubMed: 8379800]

McHugh S, Deacon R, Rawlins J, Bannerman DM. Amygdala and ventral hippocampus contribute differentially to mechanisms of fear and anxiety. Behavioral neuroscience. 2004; 118:63. [PubMed: 14979783]

Mitra R, Jadhav S, McEwen BS, Vyas A, Chattarji S. Stress duration modulates the spatiotemporal patterns of spine formation in the basolateral amygdala. Proceedings of the National Academy of Sciences of the United States of America. 2005; 102:9371–9376. [PubMed: 15967994]

Mlynárik V, Cudalbu C, Xin L, Gruetter R. 1 H NMR spectroscopy of rat brain in vivo at 14.1 Tesla: improvements in quantification of the neurochemical profile. Journal of Magnetic Resonance. 2008; 194:163–168. [PubMed: 18703364]

Noble WS. How does multiple testing correction work? Nature biotechnology. 2009; 27:1135–1137.

Næss-Schmidt ET, Blicher JU, Eskildsen SF, Tietze A, Hansen B, Stubbs PW, Jespersen S, Østergaard L, Nielsen JF. 2017Microstructural changes in the thalamus after mild traumatic brain injury: A longitudinal diffusion and mean kurtosis tensor MRI study. Brain Injury. :1–7.

Paxinos, G., Watson, C. The rat brain in stereotaxic coordinates. Qingchuan Zhuge translate)(People's Medical Publishing House; Beijing, China. 2007; 1998. p. 32

Pfeuffer J, Tkáč I, Gruetter R. Extracellular–intracellular distribution of glucose and lactate in the rat brain assessed noninvasively by diffusion-weighted 1H nuclear magnetic resonance spectroscopy in vivo. Journal of Cerebral Blood Flow & Metabolism. 2000; 20:736–746. [PubMed: 10779018]

Provencher SW. Automatic quantitation of localized in vivo1H spectra with LCModel. NMR in Biomedicine. 2001; 14:260–264. [PubMed: 11410943]

Radley J, Sisti H, Hao J, Rocher AB, McCall T, Hof P, McEwen B, Morrison J. Chronic behavioral stress induces apical dendritic reorganization in pyramidal neurons of the medial prefrontal cortex. Neuroscience. 2004; 125:1–6. [PubMed: 15051139]

Radley JJ, Rocher AB, Janssen WG, Hof PR, McEwen BS, Morrison JH. Reversibility of apical dendritic retraction in the rat medial prefrontal cortex following repeated stress. Experimental neurology. 2005; 196:199–203. [PubMed: 16095592]

Radley JJ, Rocher AB, Miller M, Janssen WG, Liston C, Hof PR, McEwen BS, Morrison JH. Repeated stress induces dendritic spine loss in the rat medial prefrontal cortex. Cerebral Cortex. 2006; 16:313–320. [PubMed: 15901656]

Rajkowska G. Postmortem studies in mood disorders indicate altered numbers of neurons and glial cells. Biological psychiatry. 2000; 48:766–777. [PubMed: 11063973]

Roozendaal B, McEwen BS, Chattarji S. Stress, memory and the amygdala. Nature Reviews Neuroscience. 2009; 10:423–433. [PubMed: 19469026]

Sacchet MD, Camacho MC, Livermore EE, Thomas EA, Gotlib IH. Accelerated aging of the putamen in patients with major depressive disorder. 2016

Sapolsky RM. The possibility of neurotoxicity in the hippocampus in major depression: a primer on neuron death. Biological psychiatry. 2000; 48:755–765. [PubMed: 11063972]

Sousa N, Lukoyanov N, Madeira M, Almeida O, Paula-Barbosa M. Reorganization of the morphology of hippocampal neurites and synapses after stress-induced damage correlates with behavioral improvement. Neuroscience. 2000; 97:253–266. [PubMed: 10799757]

Steptoe A, Kivimäki M. Stress and cardiovascular disease. Nature Reviews Cardiology. 2012; 9:360–370. [PubMed: 22473079]

Stockmeier CA, Mahajan GJ, Konick LC, Overholser JC, Jurjus GJ, Meltzer HY, Uylings HB, Friedman L, Rajkowska G. Cellular changes in the postmortem hippocampus in major depression. Biological psychiatry. 2004; 56:640–650. [PubMed: 15522247]

Surendran S, Bhatnagar M. Upregulation of N-acetylaspartic acid induces oxidative stress to contribute in disease pathophysiology. International Journal of Neuroscience. 2011; 121:305–309. [PubMed: 21348802]

Tkáč I, Henry PG, Andersen P, Keene CD, Low WC, Gruetter R. Highly resolved in vivo 1H NMR spectroscopy of the mouse brain at 9.4 T. Magnetic Resonance in Medicine. 2004; 52:478–484. [PubMed: 15334565]

Tse YC, Montoya I, Wong AS, Mathieu A, Lissemore J, Lagace DC, Wong TP. A longitudinal study of stress-induced hippocampal volume changes in mice that are susceptible or resilient to chronic social defeat. Hippocampus. 2014; 24:1120–1128. [PubMed: 24753271]

Varga Z, Csabai D, Miseta A, Wiborg O, Czéh B. Chronic stress affects the number of GABAergic neurons in the orbitofrontal cortex of rats. Behavioural Brain Research SreeTestContent1 Sree Test Content1. 2017; 316:104–114.

Veraart J, Novikov DS, Christiaens D, Ades-Aron B, Sijbers J, Fieremans E. Denoising of diffusion MRI using random matrix theory. NeuroImage. 2016; 142:394–406. [PubMed: 27523449]

Vestergaard-Poulsen P, Wegener G, Hansen B, Bjarkam CR, Blackband SJ, Nielsen NC, Jespersen SN. Diffusion-weighted MRI and quantitative biophysical modeling of hippocampal neurite loss in chronic stress. PloS one. 2011; 6:e20653. [PubMed: 21747929]

Videbech P, Ravnkilde B. Hippocampal volume and depression: a meta-analysis of MRI studies. American Journal of Psychiatry. 2004; 161:1957–1966. [PubMed: 15514393]

Vyas A, Jadhav S, Chattarji S. Prolonged behavioral stress enhances synaptic connectivity in the basolateral amygdala. Neuroscience. 2006; 143:387–393. [PubMed: 16962717]

Vyas A, Mitra R, Rao BS, Chattarji S. Chronic stress induces contrasting patterns of dendritic remodeling in hippocampal and amygdaloid neurons. The Journal of Neuroscience. 2002; 22:6810–6818. [PubMed: 12151561]

Vyas A, Pillai A, Chattarji S. Recovery after chronic stress fails to reverse amygdaloid neuronal hypertrophy and enhanced anxiety-like behavior. Neuroscience. 2004; 128:667–673. [PubMed: 15464275]

Wiborg O. Chronic mild stress for modeling anhedonia. Cell and tissue research. 2013; 354:155–169. [PubMed: 23801433]

Willner P. Validity, reliability and utility of the chronic mild stress model of depression: a 10-year review and evaluation. Psychopharmacology. 1997; 134:319–329.

Willner P. The chronic mild stress (CMS) model of depression: History, evaluation and usage. Neurobiology of stress. 2016

Wilson MA, Grillo CA, Fadel JR, Reagan LP. Stress as a one-armed bandit: Differential effects of stress paradigms on the morphology, neurochemistry and behavior in the rodent amygdala. Neurobiology of stress. 2015; 1:195–208. [PubMed: 26844236]

Xi G, Hui J, Zhang Z, Liu S, Zhang X, Teng G, Chan KC, Wu EX, Nie B, Shan B. Learning and memory alterations are associated with hippocampal N-acetylaspartate in a rat model of depression as measured by 1 H-MRS. PloS one. 2011; 6:e28686. [PubMed: 22194886]

y Palacios RD, Campo A, Henningsen K, Verhoye M, Poot D, Dijkstra J, Van Audekerke J, Benveniste H, Sijbers J, Wiborg O. Magnetic resonance imaging and spectroscopy reveal differential hippocampal changes in anhedonic and resilient subtypes of the chronic mild stress rat model. Biological psychiatry. 2011; 70:449–457. [PubMed: 21762877]

y Palacios RD, Verhoye M, Henningsen K, Wiborg O, Van der Linden A. Diffusion kurtosis imaging and high-resolution MRI demonstrate structural aberrations of caudate putamen and amygdala after chronic mild stress. PloS one. 2014:9.

Zhao L, Wang Y, Jia Y, Zhong S, Sun Y, Zhou Z, Zhang Z, Huang L. Cerebellar microstructural abnormalities in bipolar depression and unipolar depression: A diffusion kurtosis and perfusion imaging study. Journal of affective disorders. 2016; 195:21–31. [PubMed: 26852094]

Zhao YJ, Du MY, Huang XQ, Lui S, Chen ZQ, Liu J, Luo Y, Wang XL, Kemp GJ, Gong QY. Brain grey matter abnormalities in medication-free patients with major depressive disorder: a meta-analysis. Psychol Med. 2014; 44:2927–2937. [PubMed: 25065859]

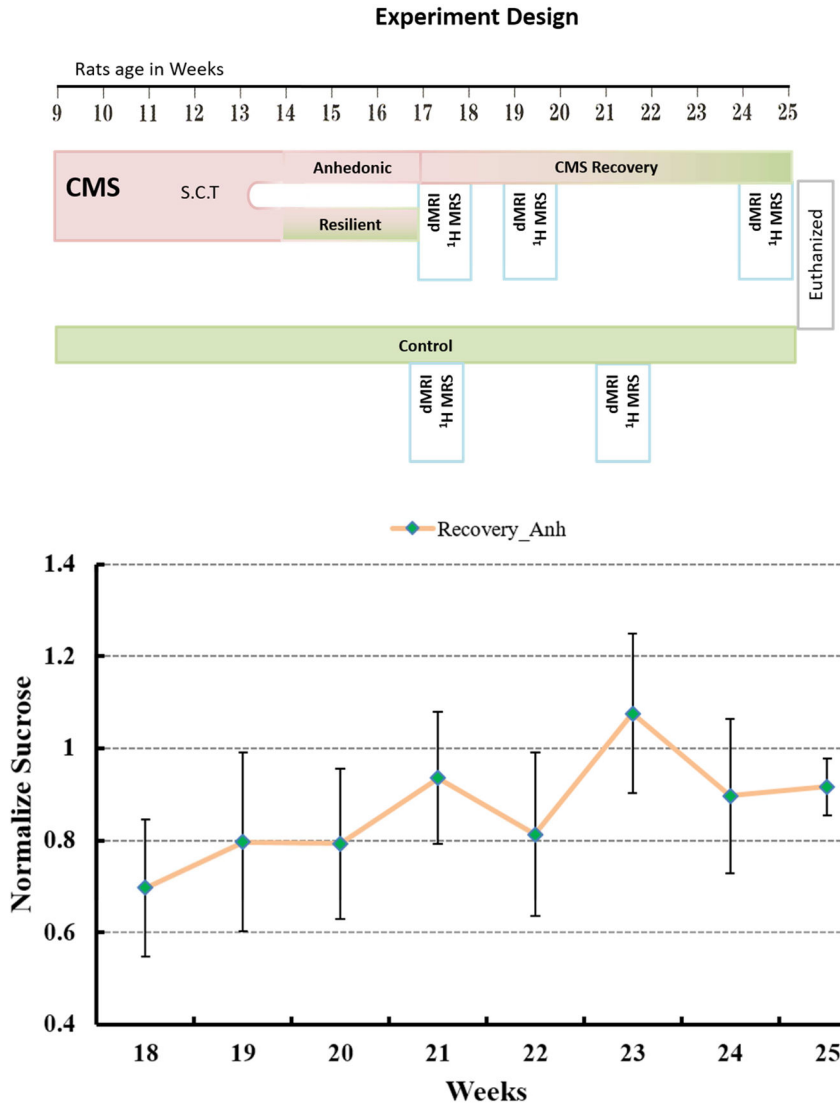

Figure 1.

Figure 1a. A group of Long-Evans rats were exposed to unpredictable chronic mild stress (CMS) from the age of 9 – 17 weeks. An age match unexposed group considered as control. CMS exposed rats were further divided into anhedonic and resilient based on sucrose consumption test (SCT). Only the anhedonic group was considered to study the recovery of microstructural and metabolic alterations. The anhedonic group was scanned longitudinally for d-MRI and ^{1}H MRS experiments at the age of week 18, week 20 and week 25. Control group was also scanned longitudinally for the same experiments at the age of week 18 and week 22.

Figure 1b. Sucrose consumption test (SCT) during the recovery of CMS indicate incremental sucrose consumption. Sucrose consumption was normalized with individual body weight and subsequently with the baseline value of SCT. A linear mixed model regression analysis shows significant group difference (***p<0.001) and significant differences at week 21 (**

p<0.01), week 23 (*** p<0.001), week 24 (* p<0.05), and week 25(** p<0.01) in comparison to the week 18 of the anhedonic group.

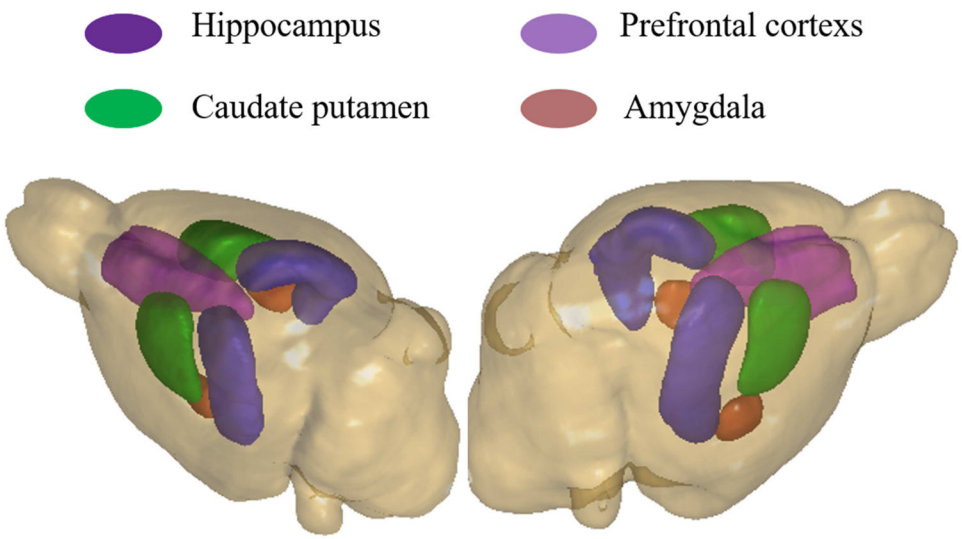

Figure 2.
A representation of rat brain and targeted region of interests (ROIs).

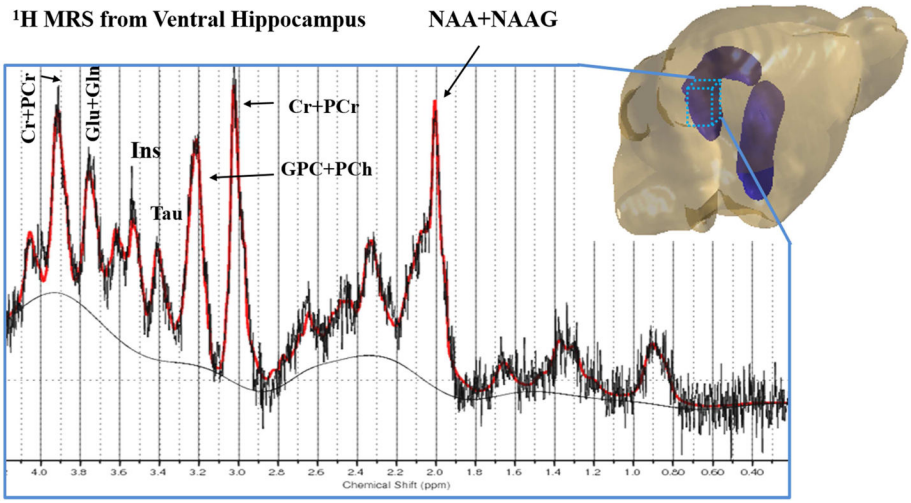

Figure 3.

^{1}H MR spectra were recorded in the left vHP with a voxel volume of ~7.5 μL (dashed line). The voxel was positioned with reference to rat brain atlas (George and Charles 1998) on a high-resolution anatomical image. A typical example of a ^{1}H MR spectrum processed on LC Model showed small metabolite peaks. Only metabolites having <20% CRLB were quantified for further statistical analysis. Seven metabolites (glutamine + glutamate (Glu +Gln), total choline (GPC and PCh), inositol (Ins), N-acetyl-aspartate (NAA), NAA + N-acetyl-aspartyl-glutamate (NAA+NAAG), glutathione (GSH), and taurine (Tau)) were analyzed and were referenced against total creatinine (Cr +PCr).

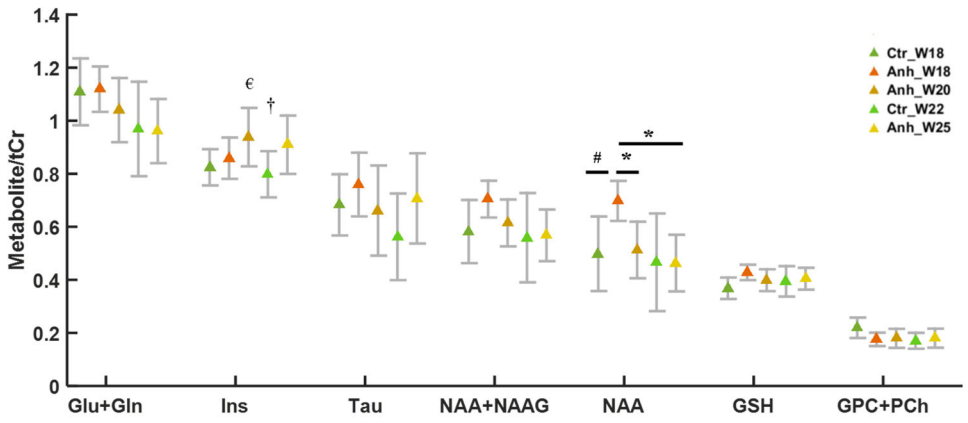

Figure 4.

Metabolites ratio with respect to total Cr (Cr+PCr) as mean ± confidence interval (CI) from the groups: control at the age of week 18 (Ctr_W18), anhedonic at the age of week 18 (Anh_W18), week 20 (Anh_W20), control at the age of week 22 (Ctr_W22) and anhedonic at the age of week 25 (Anh_W25). Linear mixed model regression analysis was performed in Matlab to compute CI. Significantly higher NAA/tCr at the age of week 18 in the anhedonic group in comparison to the control at week 18 (# $p<0.05$), and in comparison to the anhedonic at week 20 and week 25 (* p^{12}, $p^{13}<0.05$). Significantly higher value of Ins/tCr at week 20 in the anhedonic group in comparison to the mean of week 18 and week 22 of the control group (€ $p<0.05$) and the mean of week 20 and week 25 of the anhedonic group in comparison to the control at week 22 († $p<0.05$). No significant alteration was observed in the control group at the two time points.

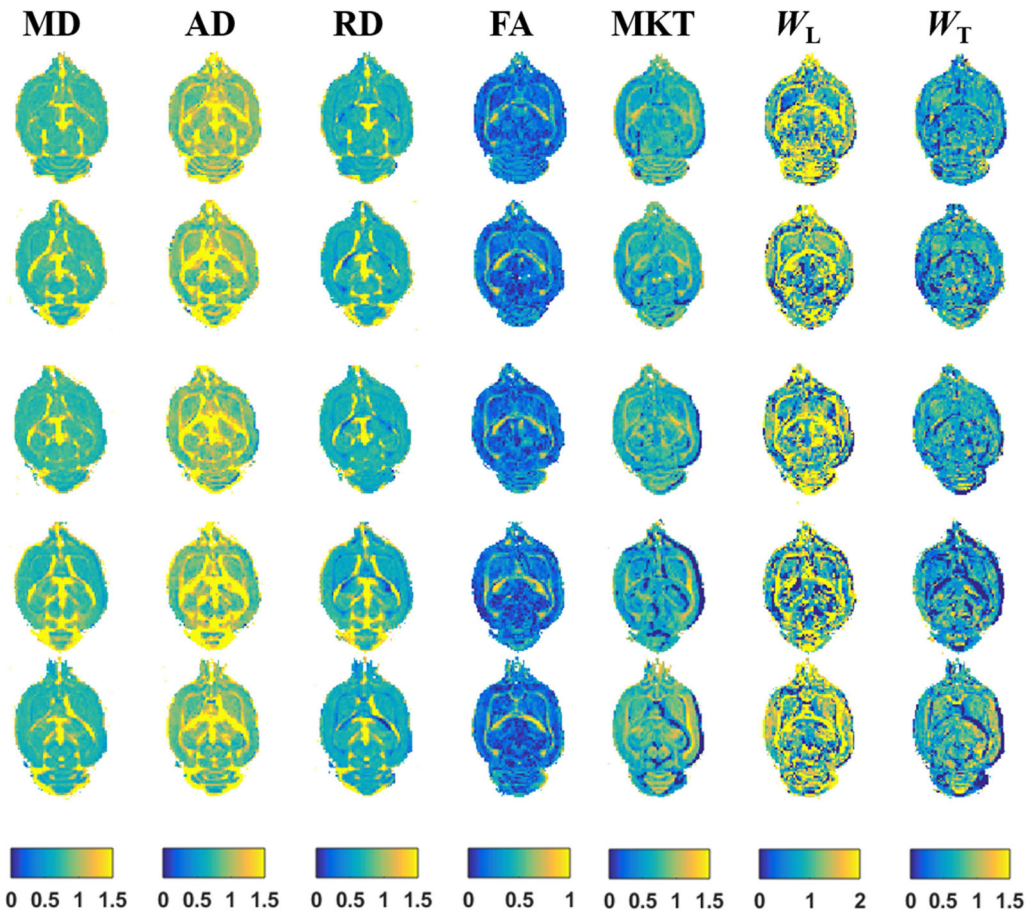

Figure 5.

Traditional d-MRI metrics (MD, AD, RD and FA), fast diffusion kurtosis metrics (MKT, W_L, and W_T) maps from control at the age of week 18 (row 1), anhedonic at the age of week 18 (row 2), week 20 (row 3), control at the age of week 22 (row 4), and anhedonic at the age of week 25 (row 5).

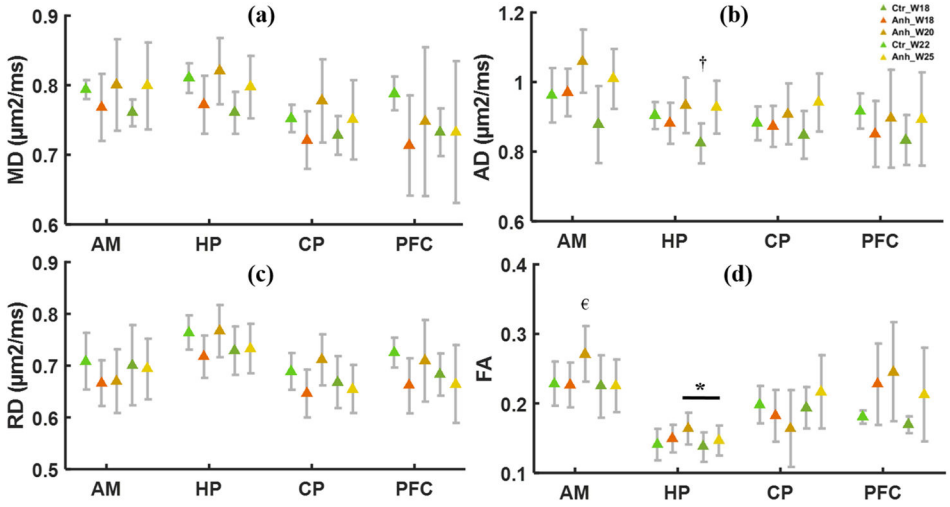

Figure 6.

(a) Mean diffusivity (MD) (µm^2/ms), (b) Axial diffusivity (AD) (µm^2/ms), (c) Radial diffusivity (RD) (µm^2/ms) and (d) Fractional Anisotropy (FA), data as mean ± confidence interval (CI) from AM, HP, CP, and PFC regions of the brain from control: green (at the age of week 18 and week 22) and, anhedonic group at the age of week 18: red, week 20: light brown and week 25:yellow. Significantly high FA was observed in AM at week 20 in the anhedonic group in comparison to the mean of control at week 18 and week 22 (€ $p<0.05$) and in the HP of the anhedonic group at week 20 in comparison to week 25 (*$p^{13}<0.05$). Significantly higher AD in HP was observed at the mean of week 20 and week 25 of the anhedonic group in comparison to the control at week 22 († $p<0.05$). No significant alteration was observed between two time points of the control group.

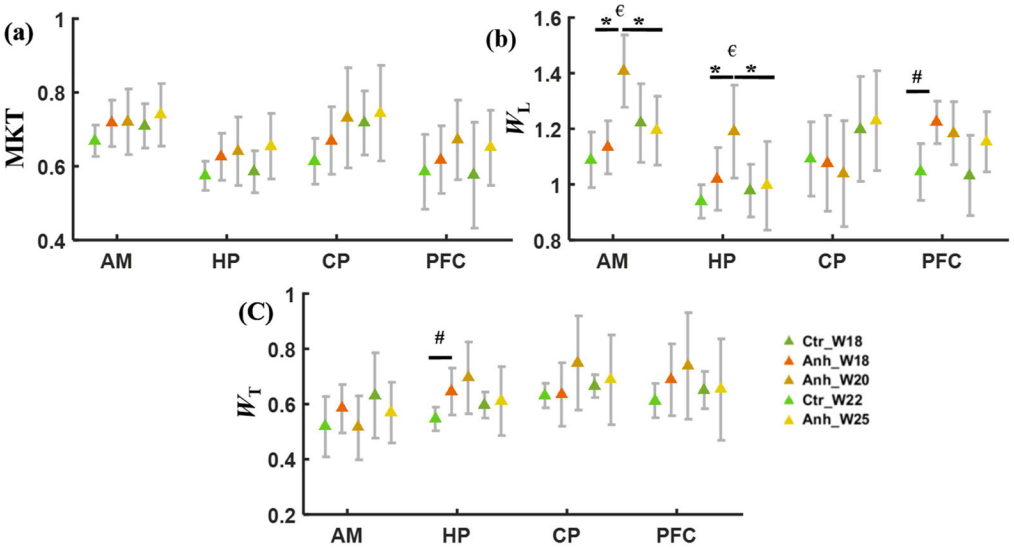

Figure 7.

(a) Mean of kurtosis tensor (MKT), (b) axial kurtosis tensor (W_L), and (c) radial kurtosis tensor (W_T) data as a mean ± confidence interval (CI) from targeted ROIs of the brain from control and the anhedonic group. Significantly higher W_L in PFC and W_T in HP (# $p<0.05$) was observed in the anhedonic group at the age of week18 in comparison to the age match control. Significantly higher W_L in AM and HP in comparison to the mean of control at week 18 and week 22 (€ $p<0.05$) and in comparison to the mean of anhedonic group at week 18 and week 25 (*p^{12}, $p^{23}<0.05$).

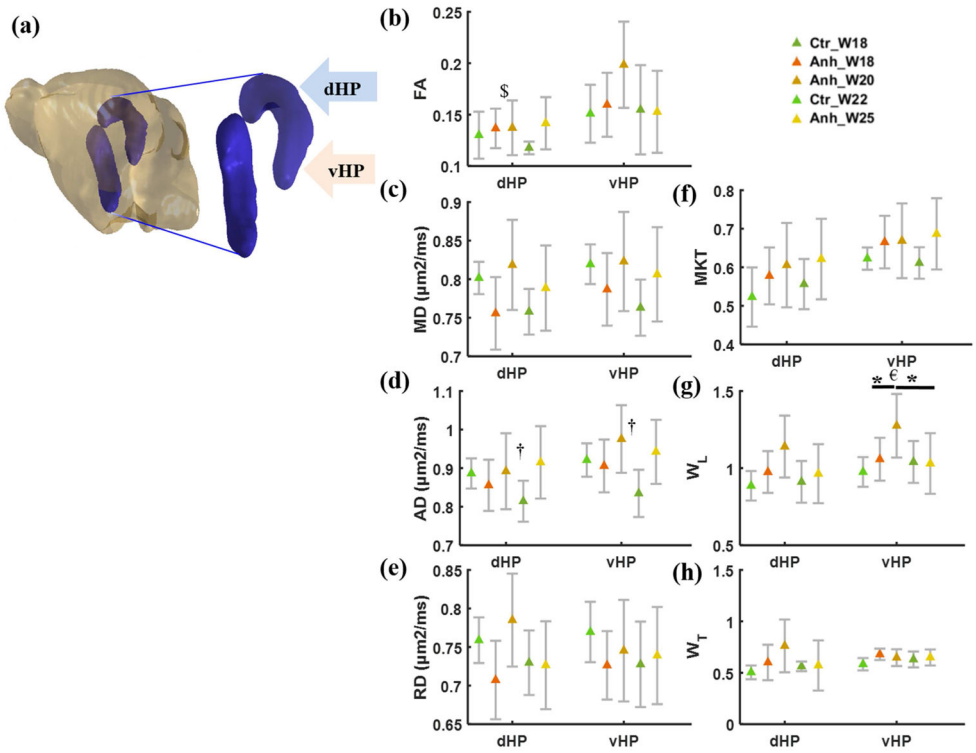

Figure 8.

(a) A representation of HP in the brain and an enlarged view of HP to further differentiate between dorsal (dHP) (−3.10 to −4.28 mm) and ventral hippocampus (vHP) (−4.60 to −8.82 relative to Bregma) with reference to brain atlas and previous literature (Christensen, Bisgaard et al. 2010, Bannerman, Sprengel et al. 2014, George and Charles 1998). (b–e) FA, MD (μm^2/ms), AD (μm^2/ms) and RD (μm^2/ms), (f–h) MKT, W_L, and W_T data as mean ± CI from dHP and vHP of the brain from control and anhedonic group. W_L shows significant increase in vHP at week 20 in the anhedonic group in comparison to the mean of week 18 and week 22 of the control group (€ $p<0.05$) and in comparison to the anhedonic group at week 18 and week 25 (*$p<0.05$). Significantly higher AD in dHP and vHP at the mean of week 20 and week 25 of the anhedonic group in comparison to week 22 control († $p<0.05$). Only FA shows significant alteration between control group at two time points in dHP ($ $p<0.05$).

Table 1

Student t-test was performed to check the level of significance between week 18 anhedonic and control (#). Linear mixed model regression analysis was performed to test the level of significance in the anhedonic group at three time points (week 18, week 20 and week 25) and significant p value (*) of post hoc t test is informed (p^{12}: significant difference between week 18 and week 20, p^{13}: significant difference between week 18 and week 25 and, p^{23}: significant difference between week 20 and week 25). A mean of control at week 18 and week 22 considered as week 20 and compared with the anhedonic group at the age of week 20 (€). Control at week 22 was compared with the mean of week 20 and week 25 of the anhedonic group (†). Paired t-test was performed to check the level of significant difference between control at week 18 and week 22 ($). Post hoc tests were performed only when there is a significant group difference in the anhedonic group. All the p values were subjected to FDR correction across all measurements.

Statistics							
Anhedonic	Week 18	Week 18	Week 20	Week 25	*Week 20*	*Week 22 mean (Week 20+Week 25)*	
		p^{12}					
			p^{23}				
		p^{13}		p^{13}			
Control	Week 18				*Week 20 mean(Week 18+Week 22)*	*Week 22*	Week 18 Vs Week 22
Test + FDR Correction	t-test **(#: p<0.05)**	Linear mixed model **(*: p<0.05)**			t-test **(€: p<0.05)**	t-test **(†: p<0.05)**	Paired t-test **($: p<0.05)**

Table 2

A summary of findings from diffusion metrics and ^{1}H MRS based metabolite levels. At week 18, W_L was altered significantly in PFC and W_T was altered significantly in HP in comparison to the age match control (#). W_L was significantly altered in AM (p^{12}, p^{23}) and HP (p^{12}, p^{23}) and FA was significantly increased in HP (p^{23}). At week 20 in comparison to mean of control at week 18 and week 22, W_L was significantly increase in AM, HP (vHP) and FA was significantly increase in AM (€). At week 22 significant alteration was observed in AD of HP in comparison to control (†). ^{1}H MRS based metabolite levels have shown significant increase in NAA at week 18 in the anhedonic group in comparison to the age match control 18 (#), and in between week 18 and week 20 (p^{12}) and week 18 and week 25 (p^{13}) of the anhedonic group. Significantly high Ins at week 20 in the anhedonic group in comparison to the mean of control at week 18 and week 22 (€) and mean of the Ins in the anhedonic group at week 20 and week 25 was significantly high in comparison to the control at week 22 (†).

	Diffusion metrics							**Metabolites/tCr (vHP)**						
Par	**AD**	**W_L**	**RD**	**W_T**	**MD**	**MKT**	**FA**	**Glx**	**Ins**	**Tau**	**NAA+ NAAG**	**NAA**	**GSH**	**GPC+ PCh**
#		PFC		HP								#		
pl2		AM, HP										*		
pl3												*		
p23		AM, HP					HP							
€		AM, HP (vHP)					AM		€					
†	HP (dHP, vHP)								†					